Available online at www.sciencedirect.com
ScienceDirect
Journal of Nuclear Materials 363–365 (2007) 287–293
journal of nuclear materials
www.elsevier.com/locate/jnucmat

Erosion and deposition in the JET MkII-SRP divertor

J.P. Coad [a,*], P. Andrew [a], S.K. Erents [a], D.E. Hole [b], J. Likonen [c], M. Mayer [d], R. Pitts [e], M. Rubel [f], J.D. Strachan [g], E. Vainonen-Ahlgren [c], A. Widdowson [a], JET-EFDA Contributors [1]

[a] *EURATOM/UKAEA Fusion Association, Culham Science Centre, Abingdon OX14 3DB, UK*
[b] *Department of Engineering and Design, University of Sussex, Brighton, East Sussex, UK*
[c] *Assoc. EURATOM-TEKES, VTT Processes, 02044 VTT, Espoo, Finland*
[d] *Max-Planck-Institut für Plasmaphysik, EURATOM Assoc., D-85748 Garching, Germany*
[e] *CRPP, Ecole Polytechnique Federale de Lausanne, CH-1015, Switzerland*
[f] *Royal Institute of Technology, Assoc. EURATOM-VR, 100 44 Stockholm, Sweden*
[g] *Plasma Physics Laboratory, Princeton University, Princeton, NJ 08543, USA*

Abstract

Carbon-13 labelled methane was injected into the outer divertor during a series of H-mode discharges on the last day of operations with the JET MkII-SRP divertor. Tiles from around the vessel were removed during the subsequent shutdown and surface deposits were analysed by IBA techniques and SIMS. First attempts to model the pattern of ^{13}C deposition using EDGE2D are reported. Erosion of W markers at the outer divertor was observed, with implications for the ITER-like wall experiment planned for JET, whilst thin film growth in the same region has been followed by the effect on infra-red measurements. The composition of thick films deposited at the inner divertor during the MkII-SRP campaign, and the migration to the inner corner of the divertor observed by a quartz micro-balance, provide further information on divertor transport.

PACS: 52.40.Hf; 52.55.Fa; 82.80.Ms; 82.80.Yc

Keywords: Erosion and deposition; Divertor; Surface analysis; Impurities; Deuterium inventory

1. Introduction

For the JET MkII-SRP (Septum Replacement Plate) operational campaigns 2001–2004, the divertor configuration was changed, by removing the septum between the inner and outer divertor channels present during the 1998–2001 MkII-GB (Gas Box) divertor campaigns, and replacing it with a simple plate. JET also operated with a wall temperature of 473 K, compared with 573 K for most of MkII-GB. Valuable information of erosion and deposition had been gained from marker tiles installed in the divertor and main chamber during the

* Corresponding author.
E-mail address: Paul.Coad@jet.uk (J.P. Coad).
[1] See the Appendix of J. Pamela et al., Fusion Energy 2004 (Proc. of 20th Int. Conf., Vilamoura, 2004) IAEA, Vienna (2004).

0022-3115/$ - see front matter
doi:10.1016/j.jnucmat.2007.01.074

MkII-GB campaign [1,2], and a new set of markers were installed in the MkII-SRP divertor for 2001–2004. These comprised a poloidal set of tiles coated with stripes of W approx 3 μm thick, and have provided new information on erosion and migration of impurities at both the inner and outer divertor. The analysis of the films in the outer divertor has been very important for specifying the W-coated tiles to be used for the ITER-like wall experiment planned for JET. In addition to analysis of the films on all tiles by ion beam analysis (IBA) techniques and secondary ion mass spectrometry (SIMS), assessment of film thicknesses by polished cross-sections has proved useful. Also, on the last day of the MkII-GB campaign, methane with the C-13 isotope (i.e. $^{13}CH_4$) had been puffed at the top of the vessel into L-mode discharges. All the ^{13}C found by surface analysis was inboard from the injection point, mostly on the inner divertor tiles [2,3]. Another $^{13}CH_4$ puffing experiment was carried out on the last day of the 2001–2004 campaign, and experimental details and first attempts at modelling the data are reported here. The campaign also included a period of operation with reversed magnetic field, which may affect the deposition observed on samples removed in 2004.

2. Results and discussion

2.1. Deposition at the inner divertor

Under normal field conditions, impurities eroded from the main chamber are swept around the scrape-off layer (SOL) and deposited where this intersects the inner divertor. Fig. 1 shows the cross-section of the MkII-SRP divertor with the positions of samples used for SIMS analysis and sectioning. The designation 1/11, for example, means Tile number 1, sample number 11. Carbon is the principal plasma impurity, with beryllium (Be) at about 8% of the carbon (averaged over the cycle from one Be evaporation to the next), and with nickel (Ni), chromium and iron from the inconel vessel wall and tile fixings at least an order of magnitude smaller. It is assumed that the flux of impurities travelling along the SOL to the divertor reflects this composition, which is close to the mean deposition found in the main chamber (e.g. on inner wall guard limiter tiles). However, carbon is released by chemical erosion from these deposits at the inner divertor and migrates to the shadowed regions at the inner divertor corner [2,4,5]. For the 2001–

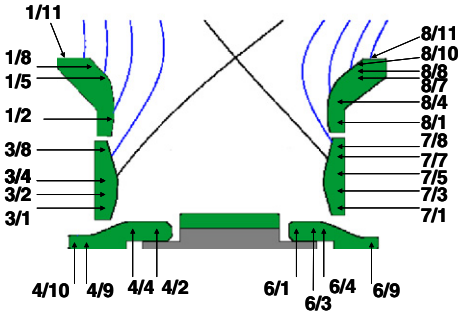

Fig. 1. Cross-section of the JET MkII-SRP divertor, showing the positions from which samples have been cut for SIMS analysis (i.e. 1/11 means Tile 1, sample number 11).

2004 campaign a Quartz Microbalance (QMB) was installed in this corner region [6]. The QMB shows that when the inner strike point is on the vertical tiles 1 and 3 there is very little deposition on the sensing crystal during exposure, and during some shots there may even be a weight loss on the crystal indicating net erosion. However, large deposition rates can be observed during shots with sweeping across the corner region. This indicates that the migration is a two-step process. Firstly, the carbon travels along field lines to form the thick deposits observed on the sloping part of Tile 4, and secondly from there it can be ejected into the shadowed region when plasma power is applied.

Following the 1999–2001 operation a duplex film structure had been found for deposits at the inner SOL, with an inner film of high Be/C, similar to that seen previously, and an outer film with much lower Be content [2]. The outer film also contained a much greater D concentration than the inner film. Fig. 2(a) shows the secondary ion mass spectroscopy (SIMS) [7] profiles for ^{12}C, ^{13}C, Be and Ni through the film on Sample 3.8, which was cut from near the top of a Tile 3 removed from JET in 2001. The Be/^{12}C ratio is much lower in the outer one-third of the film to that in the inner part of the film, and the behaviours of Be and Ni are similar. Rutherford backscattering (RBS) analysis of many samples from tiles 1 and 3 removed in 2001 gave an average composition for this outer layer of 13% Be in C [2]. This ratio is closer to the 8% Be in C found in deposits in the main chamber, implying that the chemical sputtering process for removing C from the layers is less effective. It was suggested that this might have been due to lowering the JET operating temperature from 573 to 473 K for the last three months of the campaign, or to a 2-month

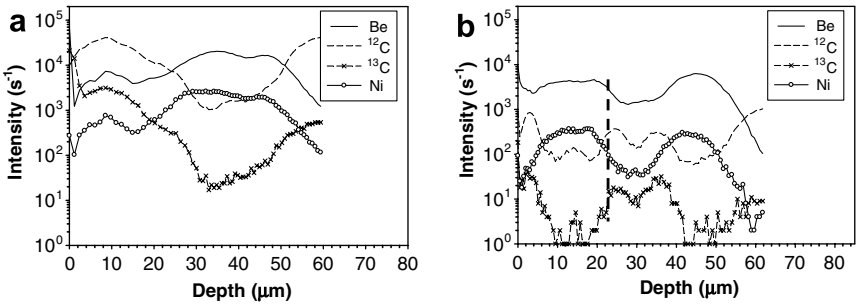

Fig. 2. (a) SIMS profile through the film on sample 3.8, from Tile 3 exposed during: (a) 1999–2001 and (b) 1998–2004.

period of He fuelling just before the end of the campaign.

JET has continued to operate at 473 K during 2001–2004, and Fig. 2(b) shows the SIMS spectrum from a similar point on a Tile 3 that had been in the vessel from 1998 to 2004. The profiles at the inner part of the film (to the right of the line drawn on the figure) are similar to those seen in Fig. 2(a) and probably correspond to film deposited in the period 1998–2001, implying the outer part corresponds to film deposited 2001–2004. The majority of the 2001–2004 deposits again contain high concentrations of Be (and other metals such as Ni). These results are confirmed by RBS as shown in Fig. 3, which shows spectra from samples 3.7 from Tile 3 removed in 2001 and from one removed in 2004. The spectrum from 2001 shows features characteristic of a predominantly ^{12}C sample, with a large deuterium (D) concentration and some oxygen. However, the spectrum from the tile removed in 2004 clearly shows less D, a large Be concentration and a larger contribution of Ni, Fe and Cr. Note that there was a clear ^{13}C peak from the 2001 tile but no ^{13}C peak is evident on the 2004 tile (see Section 2.3).

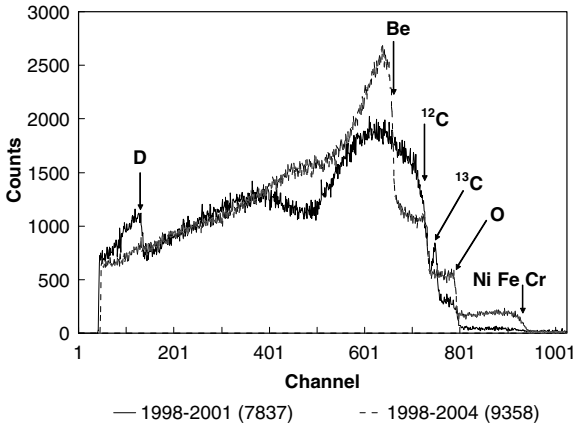

Fig. 3. RBS spectra from sample position 7 on a Tile 3 exposed in JET 1998–2001 and one exposed 1998–2004.

The Be/C ratios are comparable with the levels seen in the inner layer formed in 1999–2001 and in earlier campaigns [8]. It is clear that chemical sputtering of C at the inner divertor returned for the majority of the 2001–2004 operations from the reduced rate at the end of the 1999–2001 campaign to its earlier value, despite the similar JET wall temperature. It appears, therefore, that the reduced chemical sputtering in early 2001 results from the He-fuelled campaign. The high D content of the layer may result from the last few days of the campaign when operations reverted to D-fuelling, and may imply that the layer deposited during the He phase was of a different structure.

2.2. Erosion at the outer divertor

Tiles 7 and 8 removed in 2001 showed no net deposition, and markers had largely been eroded [1]. New divertor tiles with markers were installed in 2001 [9], and Tile 7 removed in 2004 showed a more complex picture. A vertical slice of Tile 7 that includes the W stripe is shown at the top of Fig. 4, rotated 90° so that the top of the tile is at the left-hand side. There appear to be thin deposited layers on the upper part of the tile, which were confirmed by IBA analysis, and some evidence of the 3 μm poloidal W marker stripe remained visible at all points. However, IBA and SEM analysis of the W stripe shows that up to 70% of the film has been sputtered away from the area of the tile corresponding to the most common strike point position, leaving exposed areas of the CFC surface [10]. This is towards the bottom of the tile, i.e. the right-hand side in Fig. 4. Part of the deposition occurred during the ^{13}C puffing experiments, but deposition also occurred on Tile 7 during the reverse field campaign (see next section).

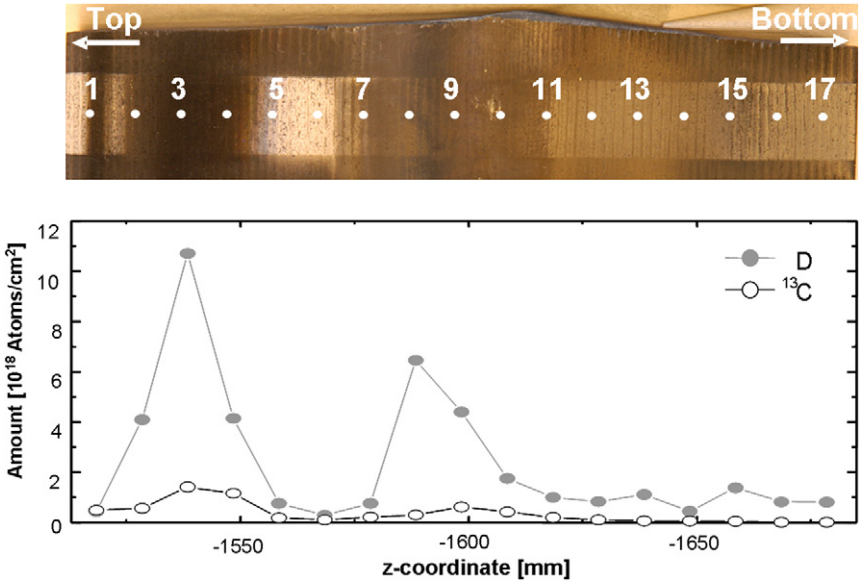

Fig. 4. D and ^{13}C concentrations plotted along the W-stripe seen in the panel above. The left-hand edge of the stripe in the picture is the top of Tile 7, the right-hand edge the bottom.

The appearance by eye of the W stripe on Tile 8 when it was removed in the 2004 shutdown was very similar to when it was mounted in 2001. However, as for Tile 7, detailed analysis of the stripe by IBA and scanning electron microscopy (SEM) has shown that the majority of the W has been eroded on the upper part of the front face of the tile and from the outer, horizontal, surface [10]. There were comparatively few discharges run with the strike point on Tile 8, so the erosion on Tile 8 remains to be explained. The observed W-erosion for Tile 7 is in general agreement with ERO modelling of the W net erosion using campaign averaged particle fluxes, and provides important data for the ITER-like wall project planned for JET [11].

2.3. Puffing experiments

$^{13}CH_4$ was puffed into the outer SOL from injection points between tiles 7 and 8, with 48 nozzles located toroidally. The amount of ^{13}C has been measured over a complete poloidal scan of the divertor, and the amounts detected are listed in Table 1 as an average for each tile. This quantity is then extrapolated toroidally around the vessel and expressed as a percentage of the amount puffed in. The total percentage is only a small fraction of the input, and less than found after the 2001 puffing [2]. Although a significant amount was found in the private flux region, it was clear that some ^{13}C was transported around the SOL, as ^{13}C was measured on a probe inserted into the SOL at the top of the machine [12]. The highest concentrations of ^{13}C have been seen in the outer SOL just above the strike-point on Tile 7 where a deposited film is clearly visible, and on the horizontal section of Tile 8. A number of possible explanations may be proposed to explain the ^{13}C on the horizontal surface. Firstly, a material transport loop for ^{13}C may be established in the SOL from the outer divertor close to the separatrix, migrating into the main chamber and returning to the far SOL. Secondly, ELMs may be responsible for the movement of ^{13}C. Thirdly, there may be a leakage path for the puffed gas from the supply manifold to the top of the outer divertor, so that gas may enter the far SOL close to the deposition site.

Table 1
Amounts of ^{13}C found on a poloidal scan of the divertor tiles, averaged over each tile, integrated toroidally and expressed as a % of the input

Tile number	^{13}C amount (%)
1	2.7
3	0.5
4	3.8
6	2.5
7	10.9
8	6.1
Total	26.5

A plot of ^{13}C concentration from top to bottom of Tile 7 is given in Fig. 4, and an RBS spectrum from the W stripe where the deposited ^{13}C is at a maximum is shown in Fig. 5. The narrow ^{12}C and ^{13}C peaks in Fig. 5 indicate a thin film comprising 1.6×10^{19} atoms cm^{-2} ^{12}C and 1.4×10^{18} atoms cm^{-2} ^{13}C on top of the remaining W film. The amount of deposited ^{13}C is similar off the W stripe, but it is not then possible to distinguish the deposited ^{12}C from that of the underlying carbon-based substrate.

The growth of a surface film was clearly seen using an infra-red (IR) camera. When there is a film on the surface and a heat pulse is applied, the surface temperature according to the IR camera increases more than if the same pulse is applied to a clean surface [13]. The ^{13}C puffing experiment was made during a series of 31 similar H-mode discharges with regular ELMs. During the discharge while the strike point is on the divertor tiles there is a steady rise in the tile surface temperature, but at each ELM there is additionally a 'spike' in the surface temperature (a fast rise to a new value and rapid return to near the initial temperature). Throughout the series of pulses the pattern of ELM spikes on the inner divertor temperature remains constant at $\Delta T = 300$ K, since there is an established thick coating over the inner divertor. However, at the outer divertor, the size of the ELM spikes increases continually through the series from $\Delta T = 50$ K to $\Delta T = 300$ K, demonstrating that the ^{13}C injection in the outer divertor turned part of the outer target into a deposition-dominated area. The IR response suggests that the majority of the surface film developed during the puffing experiment, and that the ^{12}C results from carbon self-sputtering elsewhere on the tile and re-deposition after toroidal transport.

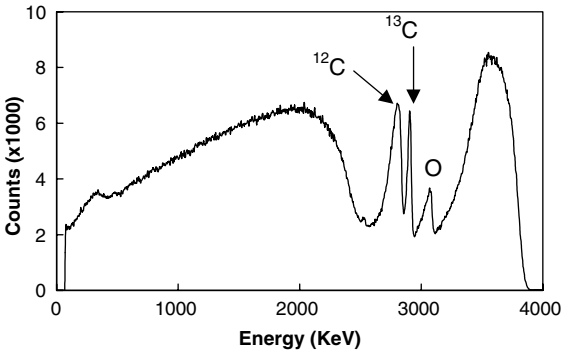

Fig. 5. RBS spectrum of the thin deposit on the W-stripe near the top of Tile 7 after exposure in JET 2001–2004 (where D and ^{13}C are maxima in this figure).

In June/July 2003 one month of JET plasma operations was devoted to experiments with reversed magnetic field. In this configuration, plasma temperature and density in the inner and outer divertor legs are more similar, and the drift velocity in the SOL from outboard to inboard seen for the normal field direction is greatly reduced [14]. The IR camera provides evidence for deposition in the outer divertor at this time. Temperature spikes for ELMs increase in magnitude in the outer divertor in a similar manner to that described above for the puffing experiment. The excess surface temperature rose to a saturation level of ~150 K/(MW m^{-2}) (similar to that in the inner divertor) in approximately 100 pulses [13]. Tile 6 and items collected from the shadowed region in the corner of the outer divertor during the 2004 shutdown also show some deposition in this region. Although comprehensive measurements have yet to be carried out, the amounts appear to be significantly less than in the inner divertor, but much greater than the negligible deposition observed here in previous shutdowns. Since the reversed field operations lasted for 4 weeks compared with 100 weeks under normal conditions, less deposition in the outer divertor is only to be expected.

Significant ^{13}C levels are found throughout the private region of the divertor, and smaller ^{13}C concentrations are found in the inner divertor SOL, as were listed in Table 1. ^{13}C in the inner divertor is believed to have travelled around the top of the machine with the deuterium SOL flow, since ^{13}C was observed on probes exposed at the top of the vessel [12]. Overall the amounts detected only account for ~26.5% of the ^{13}C that has been injected.

2.4. Modelling of the puffing

EDGE2D was used to describe the material migration from the gas injection location during the ^{13}C injection experiments. EDGE2D assumes that the carbon is injected as an atom, then follows the neutral trajectories using the Monte Carlo code NIMBUS. The carbon, once ionized is part of a fluid treatment of the SOL, core pedestal region, and private flux region. In order to identify the migration pattern of the injected carbon, then EDGE2D was run without other impurity except for the injected carbon. So the effects of sputtered carbon are ignored here in order to have a clear identification of the migration of the injected

carbon. The atomic physics package in EDGE2D/NIMBUS does not treat ^{13}C, so the migration of ^{12}C was followed instead. Furthermore the effects of re-erosion have not been considered and these may be important. The migration of ^{13}C injected from the outer divertor occurred in H-Mode plasma with 125 Hz ELMs. These ELMs were modeled using the EDGE2D ELM models developed by Kallenbach [15]. Generally, EDGE2D is better able to study the long range migration of the carbon, in this case from the outer divertor to the inner divertor.

The ELMs modeled by Kallenbach were larger than the ELMs that occurred in the ^{13}C migration experiment, being 100 kJ energy drops rather than 30 kJ. Consequently, the ELM model of Kallenbach was applied to the migration plasmas but with a reduced increase in the transport coefficients by about 20% in order to obtain the smaller energy drop induced by these ELMs. Both conductive ELMs and convective ELMs were tried, and results were similar for both cases, in that the ^{13}C migration occurred primarily inter-ELM rather than during the ELM. The reason for this was that during the ELM, the temperatures are higher in the divertor and the carbon is ionized closer to the gas inlet, and was less able to do long range migration.

Reasonable fits to the experimental ^{13}C deposition data were possible as shown in Fig. 6. The calculations have some free parameters that are not well restricted by experimental data. In this case the impurity transport coefficients in the private flux region were adjusted to be about ten times larger than in the SOL in order to obtain a good fit in the private flux region along the inner target. One flaw in the calculation is the lack of re-erosion, and it is expected that once re-erosion effects are included then a different set of private flux region impurity transport coefficients will be needed to cause the calculated deposition ('EDGE2D – PFR' in Fig. 6) to approximate the experimental data.

The calculations indicate three main migration paths with only a few percent of the injected C reaching the inner target. Firstly, EDGE2D indicates that about 98% of the injected carbon is re-deposited on the outer target. The second path is from leakage out of the outer target to the baffle top (estimated to be about 25% of the injected carbon leaving from the baffle top). Carbon is ionized in the main chamber SOL and transports the long way around the vessel to be deposited in the inner target. That deposition is displaced up the inner target away from the inner strike point, and is prevented from depositing near the inner strike point by the action of the thermal force near the entrance to the inner divertor ('EDGE2D – main SOL' in Fig. 6). Classical drifts have not been included in the calculations of this migration path, since these drifts underestimate the actual flows in the main chamber by about an order of magnitude. Rather the effects of SOL flows have been estimated by

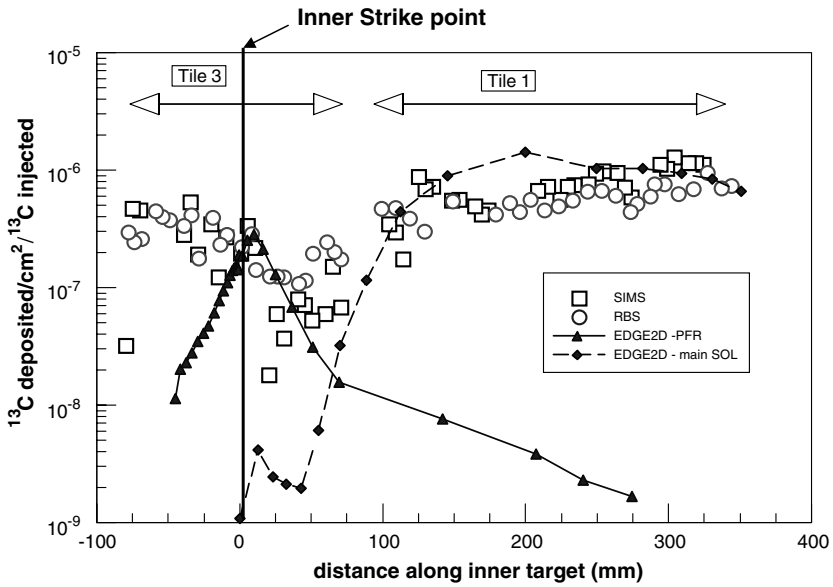

Fig. 6. Deposition (calculated and experiment) of carbon along the inner target resulting from injection near the outer strike point.

using an external force [16]. The external force was adjusted in magnitude until the main chamber SOL flow was matched. The third migration path is via the private flux region, and is caused by the action of the $E \times B$ drift in that region. In EDGE2D that drift acts only on the deuterium and not directly on the carbon, but nevertheless is effective at transporting carbon from the gas puff location (near the outer strike point) to (and below) the inner strike point.

3. Concluding remarks

Tiles and other samples have been removed from JET during the 2004 shutdown and analysed for erosion/deposition. W marker stripes at the outer divertor show ~70% erosion at the strike point regions and exposure of the underlying carbon surface. Deposits at the inner divertor wall tiles returned to the pre-2001 situation of high Be/C ratios, indicating ~90% removal of carbon from the inner divertor by chemical sputtering. A QMB at the inner corner of the divertor shows that the final step of migration to this region occurs when the strike point moves to the horizontal tile.

^{13}C puffed into H-mode discharges from the outer divertor SOL led to some local re-deposition that behaved as a surface film in IR camera measurements. Preliminary modelling of the general distribution over the whole divertor has been performed using EDGE2D, and indicates three migration paths are required to fit the data.

Acknowledgements

This work was funded partly by the UK Engineering and Physical Sciences Research Council and by the European Communities under the contract of Association between EURATOM and UKAEA. The view and opinions expressed herein do not necessarily reflect those of the European Commission.

References

[1] J.P. Coad, P. Andrew, D.E. Hole, S. Lehto, J. Likonen, G.F. Matthews, M. Rubel, J. Nucl. Mater. 313–316 (2003) 419.
[2] J.P. Coad, J. Likonen, M. Rubel, E. Vainonen-Ahlgren, D.E. Hole, T. Sajavaara, T. Renvall, G.F. Matthews, Nucl. Fusion 46 (2006) 350.
[3] R.A. Pitts, J.P. Coad, et al., Plasma Phys. Contr. Fusion 47 (2005) B303.
[4] J. Likonen, E. Vainonen-Ahlgren, J.P. Coad, R. Zilliacus, T. Renvall, D.E. Hole, M. Rubel, K. Arstila, G.F. Matthews, M. Stamp, J. Nucl. Mater. 337–339 (2005) 60.
[5] J. Likonen et al., J. Nucl. Mater., these Proceedings, doi:10.1016/j.jnucmat.2007.01.007.
[6] H.-G. Esser, V. Philipps, M. Freisinger, G.F. Matthews, J.P. Coad, G. Neill, J. Nucl. Mater. 337–339 (2005) 84.
[7] J. Likonen, S. Lehto, J.P. Coad, T. Renvall, T. Sajavaara, T. Ahlgren, D.E. Hole, G.F. Matthews, J. Keinonen, Fusion Eng. Des. 66–68 (2003) 219.
[8] J.P. Coad, N. Bekris, J.D. Elder, S.K. Erents, D.E. Hole, K.D. Lawson, G.F. Matthews, R.-D. Penzhorn, P.C. Stangeby, J. Nucl. Mater. 290–293 (2001) 224.
[9] S. Lehto, J. Likonen, J.P. Coad, T. Ahlgren, D.E. Hole, M. Mayer, H. Maier, J. Kolehmainen, Fusion Eng. Des. 66–68 (2003) 241.
[10] M. Mayer et al., J. Nucl. Mater., these Proceedings, doi:10.1016/j.jnucmat.2007.01.010.
[11] A. Kirschner, V. Philipps, J. Winter, U. Kögler, Nucl. Fusion 40 (2000) 989.
[12] M. Rubel, J.P. Coad, J. Likonen, G.F. Matthews, D.E. Hole, E. Vainonen-Ahlgren, In: 32nd EPS Conf. on Plasma Physics and Controlled Fusion, Europhys. Conf. Abstr. 29C (2006) P-2.004.
[13] P. Andrew, J.P. Coad, Y. Corre, T. Eich, A. Herrmann, G.F. Matthews, J.I. Paley, L. Pickworth, R.A. Pitts, M. Stamp, J. Nucl. Mater. 337–339 (2005) 99.
[14] S.K. Erents, R.A. Pitts, W. Fundamenski, J.P. Gunn, G.F. Matthews, Plasma Phys. Contr. Fusion 46 (2004) 1757.
[15] A. Kallenbach et al., Plasma Phys. Contr. Fusion 46 (2004) 431.
[16] J.D. Strachan et al., J. Nucl. Mater. 337–339 (2005) 25.